International Communications in Heat and Mass Transfer 61 (2015) 146–152

Contents lists available at ScienceDirect

International Communications in Heat and Mass Transfer

journal homepage: www.elsevier.com/locate/ichmt

Numerical simulation of the quenching process in liquid jet impingement☆

Jaewon Lee [a], Gihun Son [a,*], Han Young Yoon [b]

[a] Department of Mechanical Engineering, Sogang University, Seoul, South Korea
[b] Korea Atomic Energy Research Institute, Daejeon, South Korea

ARTICLE INFO

Available online 30 December 2014

Keywords:
Direct numerical simulation
Level-set method
Liquid jet impingement
Quenching

ABSTRACT

Direct numerical simulation is performed for quenching of a hot plate in liquid jet impingement. The flow and thermal characteristics associated with the quenching process, which includes film boiling in the fluid region as well as transient conduction in the solid region, are investigated by solving the conservation equations of mass, momentum and energy in the liquid, gas and solid phases. The liquid–vapor and liquid–air interfaces are tracked by the sharp-interface level-set method modified to treat the effect of phase change. The computations demonstrate that the boiling curve of wall heat flux versus temperature does not depend on the transient or steady-state heating conditions. The effects of initial solid temperature and solid properties on the quenching characteristics are quantified.

1. Introduction

Quenching of hot plates with liquid jet impingement has been widely used to control the mechanical and metallurgical properties of the plates. It is also applicable to emergency cooling of nuclear reactors. The quenching process has various heat transfer modes, such as film boiling, transition boiling, nucleate boiling and forced convection, depending on the plate temperature [1]. The present work focuses on the film boiling mode, which occurs in the initial period of quenching.

Steady-state experiments for film boiling in liquid jet impingement have the advantage in accurately extracting the temperature and heat flux on the solid surface (or wall) from the measured data inside the solid, when compared with the transient experiments which require a more complicated data analysis, such as using an inverse heat conduction technique [2]. Robidou et al. [3,4] conducted steady-state experiments of entire boiling regimes in planar water jet impingement and presented steady-state boiling curves of wall heat flux versus temperature varying the jet velocity and subcooling. Under the conditions of a jet width of 1 mm, a jet velocity of 0.8 m/s and a subcooling of 16 °C, the film boiling regime was observed to start at a wall temperature of about 450 °C. Subsequently, Bogdanic et al. [5] investigated the boiling modes using a miniaturized optical probe of 1.5 μm tip diameter. The vapor film thickness measured from the optical probe was 8 ± 2 μm under the experimental conditions of a jet velocity of 0.4 m/s and a subcooling of 20 °C.

Most of the other experimental studies for film boiling in liquid jet impingement were conducted under transient or quenching conditions [1,6–10]. Compared with the steady-state boiling curve, the transient boiling curve for a quenching process was observed to have an additional heat transfer regime, which occurs during the initial period of quenching and represents a rapid increase in the wall heat flux with decreasing wall temperature. The initial boiling regime was also reported by Li et al. [11] while investigating the effect of initial plate temperature on the water spray quenching process. The boiling curve was shown to vary with the initial plate temperature. However, this initial and transient behavior in the boiling curve possibly reflects a limitation in the experimental measurement rather than another heat transfer regime, as indicated by Hall et al. [6]. A fundamental understanding and prediction of the thermal characteristics is very important to design an efficient quenching process.

As an alternative way to further clarify the complex phenomena, direct numerical simulation (DNS) of the quenching process in liquid jet impingement without including empirical correlations was performed by several researchers [12–14]. However, their analysis was not extended to investigate the heat transfer characteristics in boiling regimes. DNS of film boiling was also conducted in numerical studies using a front-tracking method [15,16], a level-set (LS) method [17–20], a volume-of-fluid (VOF) method [21] and a volume-of-fluid level-set (VOSET) method [22], but they were limited to the pool boiling cases. Very recently, Kim and Son [23] and Lee and Son [24] applied the LS method to computations of film boiling in circular and planar liquid jets and predicted the vapor film thickness and wall heat flux in the stagnation region.

In this work, we extend the LS method to the quenching process of a hot plate in liquid jet impingement by solving the conduction equation

☆ Communicated by W.J. Minkowycz.

* Corresponding author at: Department of Mechanical Engineering, Sogang University, 35 Baekbeom-ro, Mapo-gu, Seoul 121-742, South Korea.
E-mail address: gihun@sogang.ac.kr (G. Son).

http://dx.doi.org/10.1016/j.icheatmasstransfer.2014.12.017
0735-1933/

Nomenclature

c_p	specific heat
F	fraction function
g	gravity
h	grid spacing
h_{lv}	latent heat of vaporization
H	height
L	length
$\dot{m}$	mass flux across the interface
$\mathbf{n}$	unit normal vector
p	pressure
q	heat flux
R	radius
t	time
T	temperature
ΔT	superheat, $T - T_{sat}$
$\mathbf{u}$	flow velocity vector, (u, v)
v_{lv}	$\rho_v^{-1} - \rho_l^{-1}$
V_j	jet velocity
W_j	jet width
x, y	Cartesian coordinates

Greek symbols

α	step function
κ	interface curvature
λ	thermal conductivity
μ	dynamic viscosity
ρ	density
σ	surface tension coefficient
τ	artificial time
ϕ	distance function from the liquid-gas interface

Subscripts

a	air
f	fluid
g	gas
i	initial
j	jet
l	liquid
s	solid
sat	saturation
v	vapor
w	solid surface or wall ($y = 0$)

in the solid region as well as the conservation equations of mass, momentum and energy in the liquid, vapor and air regions. The transient features of the quenching process are compared with the steady-state cases.

2. Numerical analysis

The present numerical approach is based on the sharp-interface LS formulation developed by Kim and Son [23] for film boiling in liquid jet impingement. The LS method is extended to include the conduction heat transfer in the solid. Fig. 1 shows the configuration used for simulation of film boiling in planar liquid jet impingement on a solid plate. The flow and temperature fields are assumed to be two-dimensional. The liquid–vapor and liquid–air interfaces are tracked by the LS function ϕ, which is defined as a signed distance from the interface. The positive sign is chosen for the liquid phase and the negative sign for the gas (vapor or air) phase. To distinguish the air and vapor regions, we introduce a step function α_a, which is defined as $\alpha_a = 1$ for the liquid–air region and $\alpha_a = 0$ for the liquid–vapor region.

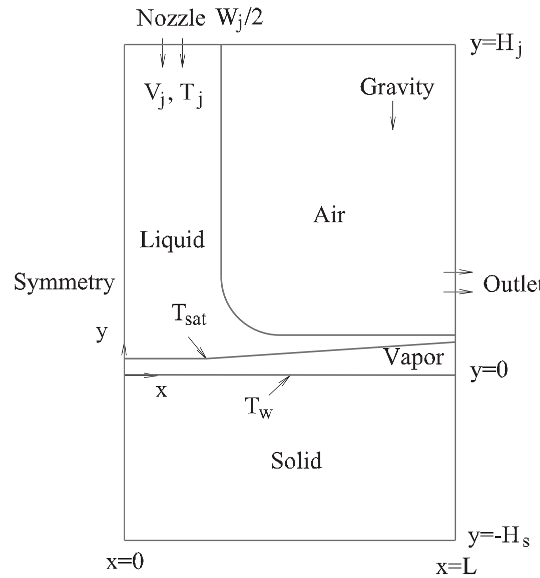

Fig. 1. Computational domain.

The conservation equations of mass, momentum and energy for the fluid (liquid, vapor or air) region ($y > 0$) are written as

$$\nabla \cdot \mathbf{u} = v_{lv}\,\dot{m}\,\mathbf{n} \cdot \nabla\alpha_l \tag{1}$$

$$\rho\frac{\partial \mathbf{u}}{\partial t} = -\left[\nabla p + \left(\sigma\kappa - v_{lv}\dot{m}^2\right)\nabla\alpha_l\right] + \nabla \cdot \mu\nabla\mathbf{u} + \mathbf{f} \tag{2}$$

$$\left(\rho c_p\right)_f\frac{\partial T_f}{\partial t} = -\left(\rho c_p\right)_f\mathbf{u}_f \cdot \nabla T_f + \nabla \cdot \lambda_f\nabla T_f \quad \text{if} \quad \alpha_a = 1 \;\text{ or }\; \phi \neq 0 \tag{3}$$

$$T_f = T_{sat} \quad \text{if} \quad \alpha_a = 0 \;\text{ and }\; \phi = 0 \tag{4}$$

where

$$\alpha_l = 1 \quad \text{if} \quad \phi > 0 \tag{5}$$

$$\quad = 0 \quad \text{if} \quad \phi \leq 0 \tag{6}$$

$$\dot{m} = (1-\alpha_a)\mathbf{n} \cdot \left[(\lambda\nabla T)_{\phi>0} - (\lambda\nabla T)_{\phi<0}\right]/h_{lv} \tag{7}$$

$$\sigma = \sigma_a\alpha_a + \sigma_v(1-\alpha_a) \tag{8}$$

$$\mathbf{n} = \nabla\phi/|\nabla\phi| \tag{9}$$

$$\kappa = \nabla \cdot (\nabla\phi/|\nabla\phi|) \tag{10}$$

$$\rho = [\rho_a\alpha_a + \rho_v(1-\alpha_a)](1-F_l) + \rho_l F_l \tag{11}$$

$$\mu^{-1} = [\mu_a\alpha_a + \mu_v(1-\alpha_a)]^{-1}(1-F_l) + \mu_l^{-1}F_l \tag{12}$$

$$\left(\rho c_p\right)_f = \left[\left(\rho c_p\right)_a\alpha_a + \left(\rho c_p\right)_v(1-\alpha_a)\right](1-\alpha_l) + \left(\rho c_p\right)_l\alpha_l \tag{13}$$

$$\begin{aligned}\lambda_f^{-1} = &\left[\lambda_a^{-1}(1-F_l) + \lambda_l^{-1}F_l\right]\alpha_a \\ &+ \left[\lambda_v^{-1}\left(1-F_\phi\right)(1-\alpha_l) + \lambda_l^{-1}F_\phi\alpha_l\right](1-\alpha_a)\end{aligned} \tag{14}$$

$$\mathbf{u}_l = \mathbf{u} + v_{lv}m\mathbf{n}(1-\alpha_l) \tag{15}$$

$$\mathbf{u}_g = \mathbf{u} - v_{lv}m\mathbf{n}\alpha_l \tag{16}$$